5-2017

Plateau Potential Fluctuations and Intrinsic Membrane Noise

Daniel Scott Borrus
College of William and Mary

Plateau Potential Fluctuations and Intrinsic Membrane Noise

A thesis submitted in partial fulfillment of the requirement
for the degree of Bachelor of Science in Neuroscience from
The College of William and Mary

by

Daniel Borrus

Accepted for _____
Honors

_____
Gregory D. Smith, Director

_____
Christy Porter

_____
Christopher Del Negro

_____

Williamsburg, VA
May 4, 2017

Daniel Borrus Thesis - Plateau Potential Fluctuations and Intrinsic Membrane Noise

Daniel Borrus
Neuroscience
Advisor: Gregory D. Smith
Department of Applied Science

May 5, 2017

Abstract

This thesis focuses on subthreshold membrane potential fluctuations in the plateau potentials of bistable neurons. Research involved with plateau potentials typically finds one of the resting membrane potentials to be more susceptible to voltage fluctuations. This difference in the amplitude of the membrane potential fluctuations is most often attributed to the voltage-dependent membrane conductance. Occasionally, however, the typically quieter resting membrane potential exhibits larger voltage fluctuations than the expected one. It has been proposed that this increased membrane potential noise is the result of the stochastic gating of the voltage-gated ion channels. In this thesis, we use a simple bistable neuron model to show that the increased intrinsic membrane noise in the quieter resting membrane potential is most likely not caused by the random gating of the ion channels.

1 Introduction

Plateau potentials can be observed in bistable neurons that exhibit two preferred resting membrane potentials (Kiehn and Eken, 1998; Wilson and Kawaguchi, 1996). In a bistable neuron, the membrane potential can jump between the two steady resting membrane potential voltages. The resting membrane potential at the higher voltage state is called a plateau potential. Figure 1 shows an example of a striatal spiny neuron switching between a low voltage resting membrane potential and a high plateau potential. This process is usually driven by subthreshold fluctuations in the neuron's membrane potential that arise from synaptic input, network phenomenon, or the intrinsic electrical properties of the neuron. In the absence of external input, the intrinsic subthreshold membrane potential fluctuations drive the transitions between "up" and "down" states. Here, the "up" and "down" states refer to the two stable resting membrane potentials at the higher and lower voltages, respectively. When membrane potential fluctuations are large enough, the membrane voltage can overcome the threshold between the two states, and move to the opposite resting potential. The size of the fluctuations in either state determines how quickly the neuron switches between the two resting potentials. Understanding what controls the sizes of the membrane potential fluctuations is crucial for understanding the behavior or the bistable neuron.

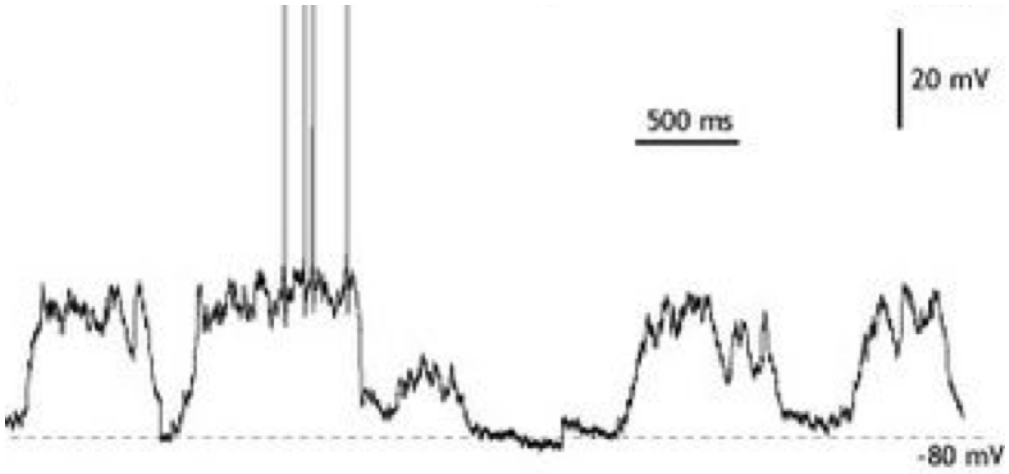

Figure 1: Example of a bistable neuron switching between a low and a high resting membrane potential. Fluctuations in the membrane potential drive the transitions between the down-state and the plateau potential. This particular neuron is a neostriatal spiny neuron. The major current responsible for the bistability is an inward-rectifying potassium current that is activated by hyperpolarization. Reproduced from Wilson and Kawaguchi (1996).

In this thesis, we look at two different factors responsible for the size of membrane potential fluctuations: (1) stochastic gating noise from the voltage-dependent ion channels and (2) voltage-dependent membrane conductance. Research involving plateau potentials has shown that the size of the fluctuations in each steady-state is typically controlled by the voltage-dependent membrane conductance, which differs for the two steady-states (Cervera et al., 2014; Hounsgaard and Kiehn, 1989; Williams et al., 1997). Occasionally, however, in experimental recordings, the size of the fluctuations observed in each state is reversed.

The steady-state that is expected to have smaller amplitude fluctuations exhibits larger fluctuations than the typically noisier steady-state. In these cases, the voltage-dependent membrane conductance cannot explain the system's behavior. It has been proposed that the increased membrane potential noise, in the typically quieter resting potential, is caused by the random gating of the voltage-dependent ion channels (Hounsgaard et al., 1988). The noise from the random opening and closing of the channels is suggested to be responsible for the unexpected increase in activity. The goal of this thesis is to determine if the random ion channel gating could actually create enough noise to overcome the ionic current interactions responsible for the voltage-dependent membrane conductance.

The rest of this thesis is organized as follows: Section 2 provides further background on plateau potentials and their fluctuations. Section 3 describes our simple bistable neuron model and the mathematical concepts involved. Sections 4 and 5 discuss the results of our simulations and the eventual conclusions we draw at the end of the thesis.

2 Background

2.1 Plateau Potentials

Plateau potentials can occur through the interaction of a passive leak current and a voltage dependent ion current. These two currents are capable of producing bistability in a neuron. One example of this is a passive leak current interacting with an inward-rectifying potassium current (Newell and Schlichter, 2005). We use current-voltage (I-V) relation graphs, such as those found in Figure 2, to explain how these two currents can create bistable membrane behavior. We also give a brief description of how to read current-voltage relation graphs. These graphs explain the intrinsic characteristics of a neuron's membrane potential and we will use them to discuss the influence of noise on the two stable resting membrane potentials.

In Figure 2, the top graph shows the leak current (I_{leak}) and the inward-rectifying potassium current (I_{Kir}) I-V relations individually. The curves represent how these currents will affect the membrane potential. In current-voltage relation graphs, a positive current value ($I > 0$) represents an outward, or hyperpolarizing current for the neuron. The hyperpolarizing current pulls the cell towards a more negative voltage value (left along the x-axis). A negative current value ($I < 0$) on the graph corresponds to an inward, or depolarizing current. Depolarization pulls the neuron toward a more positive voltage potential (right on the x-axis). The voltages where the curve crosses through $I = 0$ pA shows the current is effectively off at that voltage, and is hardly affecting the membrane potential. In this particular I-V relation, the leak current naturally pulls the membrane back to a depolarized value (≈ 0 mV), and the inward current becomes stronger as the cell becomes more hyperpolarized. We also see I_{Kir} is off during depolarization and turns on during hyperpolarization. I_{Kir} generates a hyperpolarizing current until the reversal potential for potassium (here around -85 mV). At this hyperpolarized level, the electrochemical gradient is strong enough to stop the net flow of positively charged potassium ions leaving the cell.

In order to see how the currents will interact with each other when they are in the same membrane, we can sum their two curves. This summation is shown in the bottom graph of

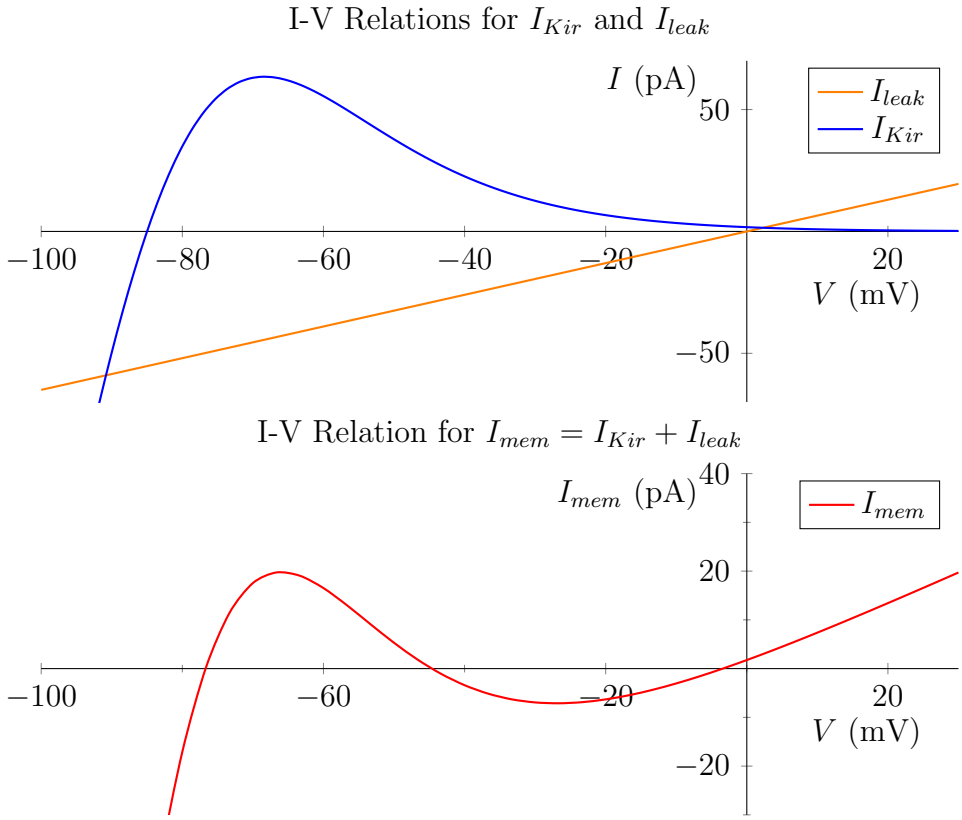

Figure 2: Top: Individual current-voltage relations for I_{Kir} (blue) and a leak current I_{leak} (orange). I_{Kir} is a voltage-gated inward-rectifying current and turns on during hyperpolarization. I_{leak} is a passive membrane current that naturally pulls the membrane towards more depolarized values. Bottom: The current-voltage relation for a membrane with both I_{Kir} and a leak current. This curve is the sum of the individual currents. The membrane potential is at a stable steady-state when $I_{mem} = 0$ pA and $I_{mem}{}' > 0$.

Figure 2. The curve of this graph (I_{mem}) represents the activity of the membrane at any voltage. Here, the voltage values where the curve crosses through $I = 0$ are steady-state voltages for the neuron's membrane potential. The neuron experiences no net current during these steady-states. If the curve passes through $I = 0$ with a positive slope, that steady-state is stable. Small perturbations away from the stable steady-state will naturally return back to the steady-state voltage. For example, if the membrane potential moves to the right, the cell will experience a hyperpolarizing current and move back towards more negative voltage values, until it reaches the steady-state again. When the curve passes through $I = 0$ with a negative slope, the reverse behavior is observed and that steady-state is unstable. Here, even the smallest perturbations result in changes in I_{mem} that cause the voltage to move away from the steady-state in either direction. In reality, it would be nearly impossible for the membrane potential to actually stay at the unstable steady-state for very long. In our example of a neuron with I_{Kir} and a leak current, there are two stable steady-states and one unstable steady-state. The two stable steady-states correspond to the two stable resting membrane potentials for the bistable neuron. The unstable steady-state represents

a threshold voltage. Fluctuations in the membrane potential would need to overcome this threshold voltage in order to jump to the opposite state. From this figure, we have insight into the exact resting membrane potential voltages, the threshold voltage for state transitions, and the origins for the bastibility. We also know the membrane potential's behavior for any initial voltage.

2.2 Ionic Currents Influence on Membrane Fluctuations

The current-voltage relation graphs can also illustrate the intrinsic properties of the resting membrane potentials, and their susceptibility to voltage fluctuations. Voltage fluctuations can arise in a number of ways, including as any form of current injection into the neuron. When external current is injected, the two resting membrane potentials respond to the external input differently. This gives rise to different fluctuation amplitudes in the two membrane potentials. To understand how this happens, let's look back at Figure 2. We can see that a neuron with this pair of currents has two stable steady-states, and therefore two resting membrane potentials. However, these steady-states are not exactly the same. The slope of the line running through the stable steady-states is very different. The slope of the curve in the current-voltage relation graph corresponds to the conductance of the cell at that voltage. (This can be realized by examining Ohm's law, $I = gV$, where g is the conductance measured in units siemens (S).) In the $I_{Kir} + I_{leak}$ system, the up-state has a lower conductance relative to the down-state.

We can simulate injecting current into the neuron by shifting the current voltage curve along the y-axis. When we shift the I-V curve for the membrane up and down, the steady-state with the low-conductance slope shifts along the x-axis much further than the steady-state with the high-conductance slope. These larger shifts along the x-axis correspond to larger changes in the stable resting membrane potential for that state. A shorter shift means current injection at that voltage has less of an effect on the membrane potential, and therefore creates smaller fluctuations. As an example, we perturb the $I_{Kir} + I_{leak}$ curve, recreated in Figure 3. Current injected into the neuron shifts the I-V relation curve up. In this scenario, the down-state, or the high-conductance state, shifts less along the x-axis than the up-state, or low-conductance state, does. Biologically, this represents the down-state's insensitivity to external current injection, and the up-state's susceptibility to external current injection. Equivalent input to both steady-states will produce larger voltage responses in the up-state.

2.3 Voltage-gated Channels and Membrane Noise

The other source for membrane potential fluctuations arises as channel noise from a voltage-dependent ion current (Chow and White, 1996; White et al., 2000). The channels in the voltage-dependent ion current are intrinsically noisy due to their stochastic gating behavior. If the number of ion channels was infinite, the fraction of channels open at steady-state could be perfectly determined by the membrane potential. This is how the gating variable is often mathematically modeled and it is called a deterministic rate model. In reality, the number of channels for a particular ion current is finite. This leads to an imbalance between the actual number of ion channels open at steady-state and the number of ion channels that are open on average for the same steady-state. This mismatch is represented in Figure 4.

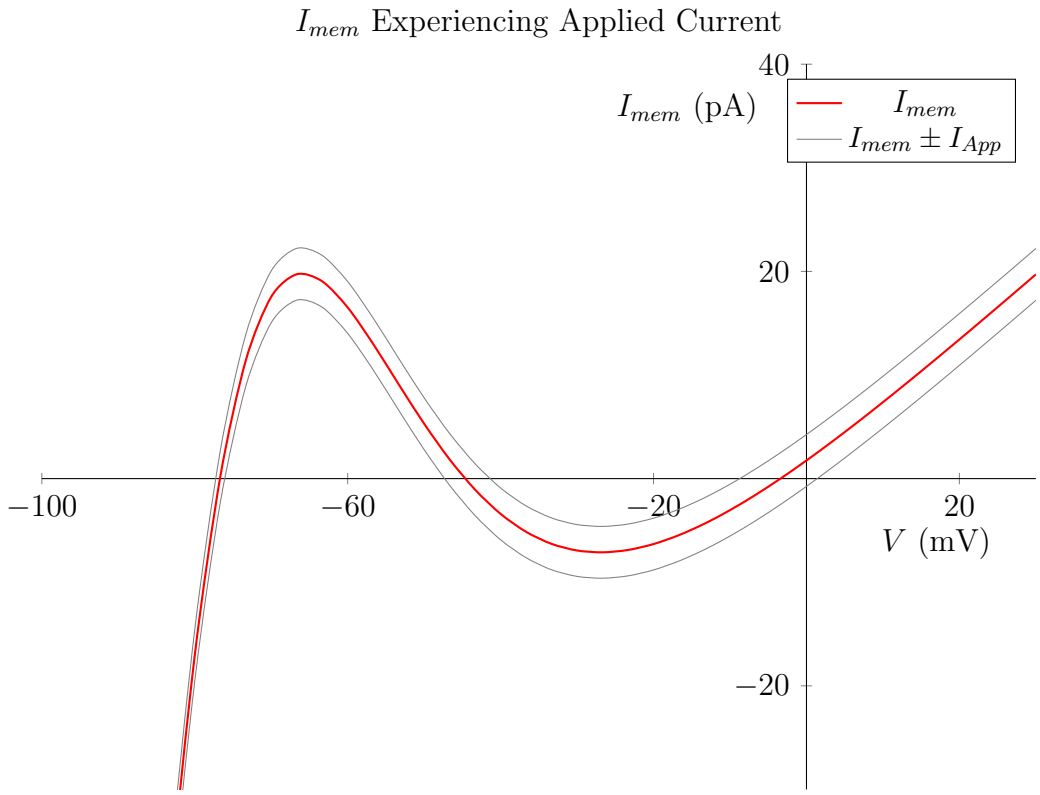

Figure 3: Current-voltage relation for the combined I_{Kir} and I_{leak}, showing the effects of external input on the two stable steady-states. When current is injected, I_{mem} shifts vertically. The steady-state voltages shift disproportionately along the x-axis. The lower conductance steady-state (the up-state) experiences much larger steady-state fluctuations than the high-conductance steady-state (down-state).

The random opening and closing of the finite number of channels causes the fraction of open channels to move above and below the deterministic amount. The channel's random behavior is described as stochastic, where each channel has a certain probability of changing states (opening or closing) depending on the membrane potential. This random channel noise, intrinsic to the voltage-gated currents, becomes larger as the number of channels decreases (Keizer, 1987). With fewer channels, the impact one channel has on the total fraction of channels open increases. This concept of intrinsic stochastic channel noise is included in our neuron model, and plays a roll in our analysis of fluctuation amplitudes for the different resting membrane potentials.

The amount of internal channel noise is also unevenly distributed across different membrane potential voltages, and it is therefore not symmetric for the two resting membrane potentials. The channels in the voltage-dependent ion current are sensitive to different voltage potentials. More specifically, they are sensitive to a range of voltage potentials, but not others. At voltage potentials outside the sensitive range, the channels mostly remain in one state (open or closed). The variance in the fraction of open channels here is small. When the membrane potential is in the middle of the channel's potential range, each channel has a 50% chance of being open, and the variance in the fraction of open channels will be

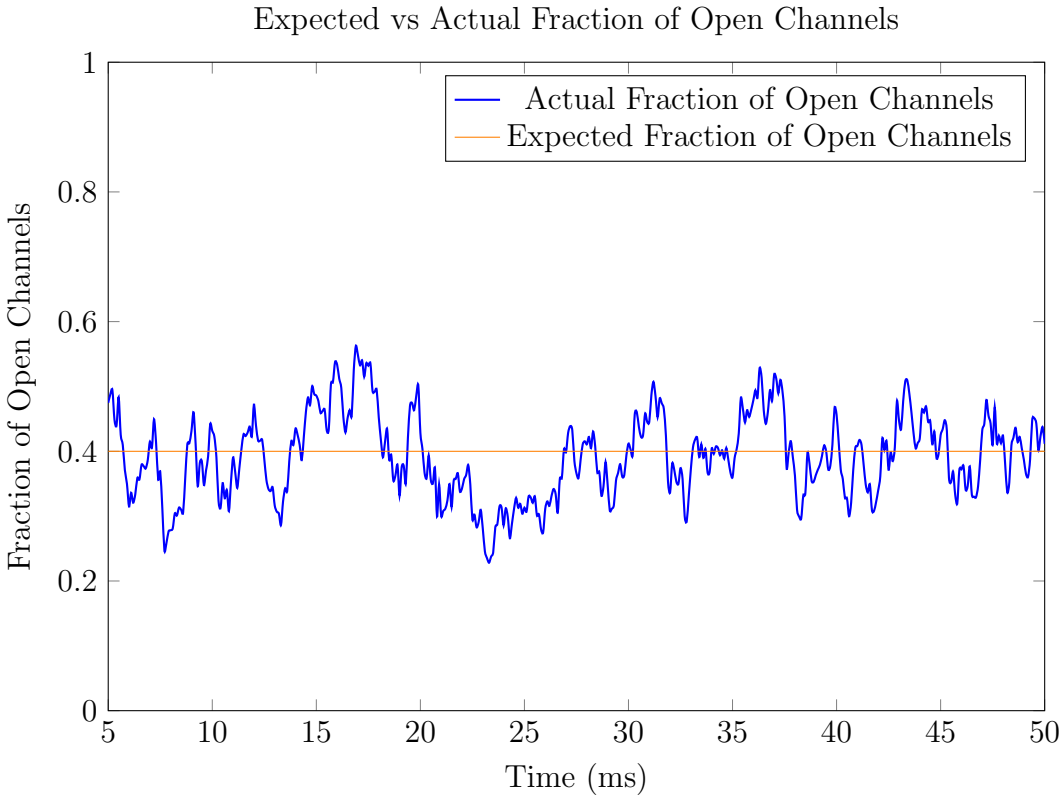

Figure 4: An example of the stochastic ion channel noise compared to the deterministic solution for the fraction of open channels at steady-state. In this example when the neuron is at steady-state, the fraction of open voltage-gated channels on average is equal to 40%. However, at any particular time, the actual fraction of open channels fluctuates around 40%. The variance in the fraction of open channels decreases as the number of total channels increases. With infinite channels, the variance in the actual fraction of open channels would be 0.

large. Channel noise will be larger during that membrane potential, and there will be larger fluctuations in the membrane potential as a result.

The previous paragraph discusses how the variance in the fraction of open channels is different for different membrane potentials, but membrane potential fluctuations also have different effects on the channel noise at different membrane potentials. When there are voltage fluctuations outside the channel's sensitive voltage range, the fraction of open channels remains relatively unaffected. But, when the same size voltage fluctuations occur inside the channel's sensitive voltage range, the fraction of open channels responds with larger fluctuations of their own. This is another reason for disproportionate channel noise at different membrane potentials.

In our example, the inward-rectifying potassium current is a voltage-gated potassium current that is activated by hyperpolarization. Refer to Figure 5 for the relationship between the membrane potential and the fraction of open I_{Kir} channels. The plateau potential in the bistable system has a resting membrane potential around 0 mV. Voltage fluctuations of ± 10 mV at the plateau potential would have a very small effect on the number of open channels.

The fraction of open channels remains close to 0 for voltage fluctuations of that size in the up-state. There would therefore be less channel noise, and less impact on the membrane potential of the neuron. Compare this to the down-state resting membrane potential, at around −80 mV. Voltage fluctuations of ±10 in this voltage range would have a much larger impact on the fraction of open channels. This would create more channel noise, and more membrane potential fluctuations as a result. This example shows how membrane potential fluctuations can create different amounts of channel noise depending on the cell's membrane potential and the channel's sensitive voltage range.

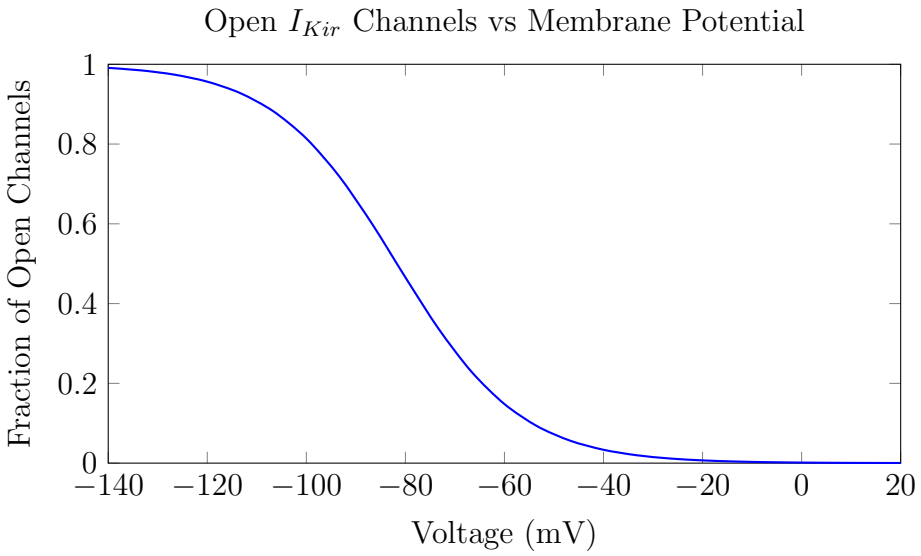

Figure 5: For I_{Kir}, the fraction of open voltage gated ion channels relative to the cell's membrane potential. I_{Kir} "turns on" as the membrane becomes more hyperpolarized. Steady-states for the bistable neuron are around −80 mV and 0 mV. With a finite number of channels, the actual number of open channels at any given time varies around the expected deterministic amount. The variance in the actual fraction of open channels is larger during the down-state. Additionally, membrane potential fluctuations cause larger shifts in the fraction of open channels during the down-state than during the up-state. These factors create more internal channel gating noise in the down-state.

In our example of a neuron containing just the $I_{Kir} + I_{leak}$ currents, we have discussed two factors that control membrane potential fluctuation amplitudes. The fluctuations created and propagated by the internal channel gating noise are larger in the down-state, where the fraction of open channels has a larger variance. Conversely, the interactions between the two ionic currents I_{Kir} and I_{leak} creates larger fluctuations in the up-state, where the low-conductance plateau potential is more susceptible to voltage fluctuations. Typically, researchers studying plateau potentials find larger membrane fluctuations during the low-conductance state (Cervera et al., 2014; Hounsgaard and Kiehn, 1989; Williams et al., 1997). The intrinsic ionic currents behind the voltage-dependent membrane conductance dominate the fluctuations caused by the stochastic ion channel gating noise. Occasionally, however, researchers find larger fluctuations in the high-conductance state. It has been proposed that this counterintuitive behavior is the result of the stochastic ion channel gating noise that

is present in the down state (Hounsgaard et al., 1988). We use a mathematical model of a simple bistable membrane with I_{Kir} and a leak current to recreate this problem, in order to determine whether or not channel noise could be responsible for the larger fluctuations in the high-conductance state.

3 The Kir Model

We implement a simple bistable neuron model to investigate the different sources of fluctuations in the resting membrane potentials. Our neuron model uses Hodgkin-Huxley type membrane balance equations to simulate a neuronal voltage trace. We only require two currents, the inward-rectifying potassium current (I_{Kir}) and the leak current (I_L). It should be noted that our model lacks any components to elicit the classic action potential. Although bistable neurons can and do fire action potentials, we are only interested in the subthreshold potentials and their fluctuations. Our model also incorporates a Langevin equation for the stochastic voltage-gated ion channels of the inward-rectifying potassium current. This is the component responsible for the channel noise.

3.1 The Hodgkin-Huxley Type ODEs

The ordinary differential equations (ODEs) for the neuron membrane potential take the form of the Hodgkin-Huxley type current balance equation (Hodgkin and Huxley, 1952):

$$C\frac{dv}{dt} = I_{app} - I_L(v) - I_{Kir}(v, m) \tag{1}$$

where,

$$I_L = g_L(v - E_L), \tag{2}$$

and

$$I_{Kir} = g_{Kir}m(v - E_{Kir}). \tag{3}$$

In these equation, C is the membrane capacitance, I_{app} is an applied current, g_L is the conductance for the leak current, g_{Kir} is the maximum conductance for the inward-rectifying potassium current, E_L is the reversal potential for the leak current, E_{Kir} is the reversal potential for potassium, and m is the fraction of open I_{Kir} channels. Note that Equations (2) and (3) are current-voltage relations and are the same equations used to create the curves in Figure 2.

The gating variable for the potassium current, m, is a "slow" variable that must be described with another ODE. In the Hogdkin-Huxley type current balance equation, the gating variable is typically modeled with a continuous and deterministic rate function. This equation takes the form:

$$\frac{dm}{dt} = -\frac{m - m_\infty(v)}{\tau_m} \tag{4}$$

where the voltage-dependent steady-state is

$$m_\infty = \frac{1}{1 + \exp(\frac{V - V_\theta}{V_1})}. \tag{5}$$

In these equations, τ_m is the characteristic time constant, and V_θ and V_1 are parameters for the location and scale of the voltage-gated ion channel curve (Figure 5). In our model we extend the modeling framework of the equation, in particular to incorporate the stochastic gating of the finite channels. See Section 3.2.

3.2 The Stochastic Gating of the Kir Channels

The m in the I_{Kir} equation corresponds to the fraction of open channels. We need to rewrite the equation for m (4) to include a stochastic noise term that will act as the random channel gating noise in I_{Kir}. We can do this by modeling the fraction of open ion channels as a continuous-time stochastic process (Smith, 2002). In I_{Kir}, the probability of a channel changing its current state (e.g., going from open to closed) depends on the cell's membrane potential. So in our model, m will be a function of the voltage: $m(v)$, and m will range from 0 to 1 because it is the number of open channels over the number of total channels. To construct our function for m we begin by examining a two state Markov chain, with states open and closed. Consider the system:

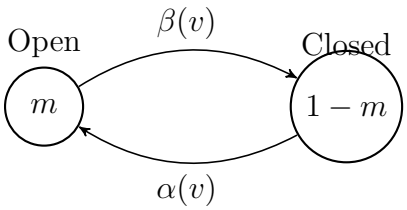

If the fraction of channels open is m, then the fraction of closed channels is $1-m$. Channels open at the rate $\alpha(v)$, and close at the rate $\beta(v)$. Both of these rates are functions of the voltage of the cell at a particular time because the channels are voltage gated. We can describe the behavior of this system with the stochastic ODE:

$$\frac{dm}{dt} = \alpha(v)(1-m) - \beta(v)m + \xi(t). \tag{6}$$

This differential equation is from the perspective of the open state. Channels enter the open state at the rate $\alpha(v)$ multiplied by the fraction of channels in closed state. Channels leave the open state at the rate $\beta(v)$ multiplied by the fraction of channels in the open state. $\xi(t)$ is the stochastic component for the ODE and is modeled after Gaussian white noise.

As mentioned before, for a deterministic system the fraction of open I_{Kir} channels as a function of voltage can be described with equations (4) and (5). We would like to rewrite equations (4) and (5) in the stochastic equation form we found above (6). Therefore, we need to find the relationship between $\alpha(v)$ and $\beta(v)$ and $m_\infty(v)$ and τ_m. We know both ODEs describe the same thing, the change in m over time. So, we can rewrite both equations slightly and compare them:

$$\frac{dm}{dt} = -\frac{m - m_\infty(v)}{\tau_m} = -\frac{1}{\tau_m}m + \frac{m_\infty(v)}{\tau_m}$$

$$\frac{dm}{dt} = \alpha(v)(1-m) - \beta(v)m = -[\alpha(v) + \beta(v)]m + \alpha(v)$$

From here, we can see similarities on the RHS of both the equations. Now, we can choose to substitute:

$$\frac{1}{\tau_m} = (\alpha(v) + \beta(v)), \text{ and}$$
$$\frac{m_\infty(v)}{\tau_m} = \alpha(v).$$

Solving for $\alpha(v)$ and $\beta(v)$:

$$\alpha(v) = \frac{m_\infty(v)}{\tau_m} \tag{7}$$
$$\beta(v) = \frac{1 - m_\infty(v)}{\tau_m}. \tag{8}$$

These are the functions that will act as the deterministic rate components of our ODE for m.

In equation (6), ξ(t) represents the stochastic component that will drive the gating noise in the fraction of open channel. ξ(t) is a rapidly varying random function of time with a normal distribution. This type of random walk is also known as a Wiener Process (Higham, 2001). This particular random walk has certain conditions that must be satisfied. First, the mean of the function at any time should be 0,

$$\langle \xi(t) \rangle = 0.$$

Second, the variance of the function should be directly proportional to time,

$$\langle \xi(t) * \xi(t') \rangle = \gamma(v)\delta(t - t').$$

The last condition also ensures that two ξ values at different times will be completely uncorrelated. When Equation (6) is combined with the stochastic noise term $\xi(t)$ it is known as the Langevin equation (Fox, 1997; Wang et al., 2015). The equation for the Wiener process in the Langevin equation can be written as:

$$\xi(t) = \sqrt{\frac{\gamma(v)}{\Delta t}} X, \tag{9}$$

where X is a standard normal random variable (mean 0 and variance 1). During the simulations, a new X is selected at every time step. Δt is the size of the time step taken by the solver (Section 3.3). In Equation (9), $\gamma(v)$ is proportional to the variance of the noise and is given by,

$$\gamma = \frac{\alpha(v)(1 - m) + \beta(v)(m)}{N} \tag{10}$$

where N is the number of channels. It is worth noting that, in this equation, as N decreases, the variance of the noise increases (Keizer, 1987). This idea of an inverse relationship between the number of channels and internal noise was discussed in section 2.3 and is incorporated into our model here.

We can now construct our equation for $\frac{dm}{dt}$ with equations (5), (6), (7), (8), (9), and (10):

$$\frac{dm}{dt} = \alpha(v)(1-m) - \beta(v)m + \xi(t) \text{ where,}$$
$$\alpha(v) = \frac{m_\infty(v)}{\tau_m},$$
$$\beta(v) = \frac{1-m_\infty(v)}{\tau_m},$$
$$m_\infty = \frac{1}{1+\exp(\frac{V-V_\theta}{V_1})}$$
$$\xi(t) = \sqrt{\frac{\gamma(v)}{\Delta t}}X \text{ and}$$
$$\gamma = \frac{\alpha(v)(1-m)+\beta(v)(m)}{N}.$$

This completes our description of the two ODEs we use to simulate the bistable neuron.

3.3 The Solver

We used Matlab R2016b to create our model. The code itself can be found in the Appendix A.1. We use Euler method to numerically integrate the ODEs given initial values for v and m. Euler method is a first-order numerical ODE solving method. The global error of the method grows proportionally with the step size, so it is vitally important to use a small step size when implementing the algorithm.

3.4 Initializing Parameters

We used the inward-rectifying potassium current model from (Newell and Schlichter, 2005) as a reference for the Kir model parameters. The I_{Kir} reversal potential is $E_{Kir} = -85$ mV. The maximum current conductance is $g_{Kir} = 15$ pS. The shaping paramater for the channel gating curve is $V_1 = 12.4$ mV and the voltage when the conductance is half maximal is $V_\theta = -81.7$ mV. See Figure 2 for the I_{Kir} current-voltage relation curve and Figure 5 for the open channel probability curve (5). τ_m is set to 1 ms. The capacitance of the cell is set to $C = 10$ pF.

We chose leak parameters to fit well with the potassium current. Typically, the leak current pulls the membrane to a depolarized voltage potential. The strength of the leak current through the membrane is the combination of many factors in the cell, and can be modulated to influence the activity of the cell, including bistability (O. Kiehn et al., 1998). For our leak current, we vary the conductance around $g_L = 0.65$ pS and the reversal potential around $E_L = 0$ mV (Figure 2).

The number of channels began at $N = 80$. However, this parameter is varied more often due to the interesting and large scale affect the number of channels has on the model. The initial values for v and m are -90 mV and $m_\infty(-90)$ for the down-state simulation respectively, and 10 mV and $m_\infty(20)$ for the up-state simulation respectively. Lastly, the time steps used are $\Delta t = 0.1$ ms.

4 Results

4.1 Initial Findings

Our initial simulation can be seen in Figure 6. The voltage and the fraction of open channels are plotted against time. The size of the fluctuations in each state is calculated by finding the variance of each voltage trace. Figure 7 shows a histogram of the v and m data, as well as a phase plane analysis of our two ODE system.

With the parameters mentioned in the previous section, our simulations showed a greater amplitude in the membrane fluctuations in the up-state or low-conductance state. This suggests that in our model, the voltage-dependent membrane conductance plays a larger role in the membrane potential voltage than the internal channel noise does. This idea was supported when we observed the proportion of open channels over time. The fraction of open channels had a higher variance in the high-conductance state (down-state) than in the low-conductance state (up-state), as we predicted. However, this large channel noise was not enough to overcome the high-conductance state's insensitivity to fluctuations. In our initial runs, the high channel noise in the down-state was dampened by the high-conductance slope. In the up-state, the small amount of channel noise, along side the up-state's susceptibility for voltage fluctuations, caused a much larger distribution in the membrane potential voltage. These results are in line with the experimental data for plateau potential fluctuations. In most cases, voltage fluctuations are larger in the low-conductance state. We showed that, in our initial run, ion channel noise was not enough to cause larger fluctuations in the high-conductance state.

4.2 Parameter Studies

In order to investigate whether or not internal channel noise can create larger fluctuations in the high-conductance state, we range several parameters in our system, over realistic ranges, in an attempt to create the opposite of our initial findings.

4.2.1 Ranging The Leak

We begin by ranging the leak parameter. We exaggerate the strength of the leak conductance by increasing the parameter g_{leak}. This increases the slope of the leak current and brings the conductance branches of the two steady-state to similar values. This makes the difference between the two steady-state membrane potential's susceptibility to membrane noise less pronounced. This allows the I_{Kir} channel noise to play a larger role in the amplitude of the membrane fluctuations. One example of our results from the leak conductance parameter study is shown in Figure 8. We tried several leak conductances ranging from g_{leak} = .55 pS to g_{leak}=.80 pS. We found that the voltage variance was always higher in the up-state and just ranging the leak alone was not enough to affect the fluctuation size of the stable resting membrane potentials to a large enough extent. It is important to note that during these parameter studies, the amount of channel noise in each resting membrane potential remains largely unaffected. The actual steady-state voltage for the resting potential shifts only slightly along the x-axis, and as a result there is not a large change in the variance of the channel noise.

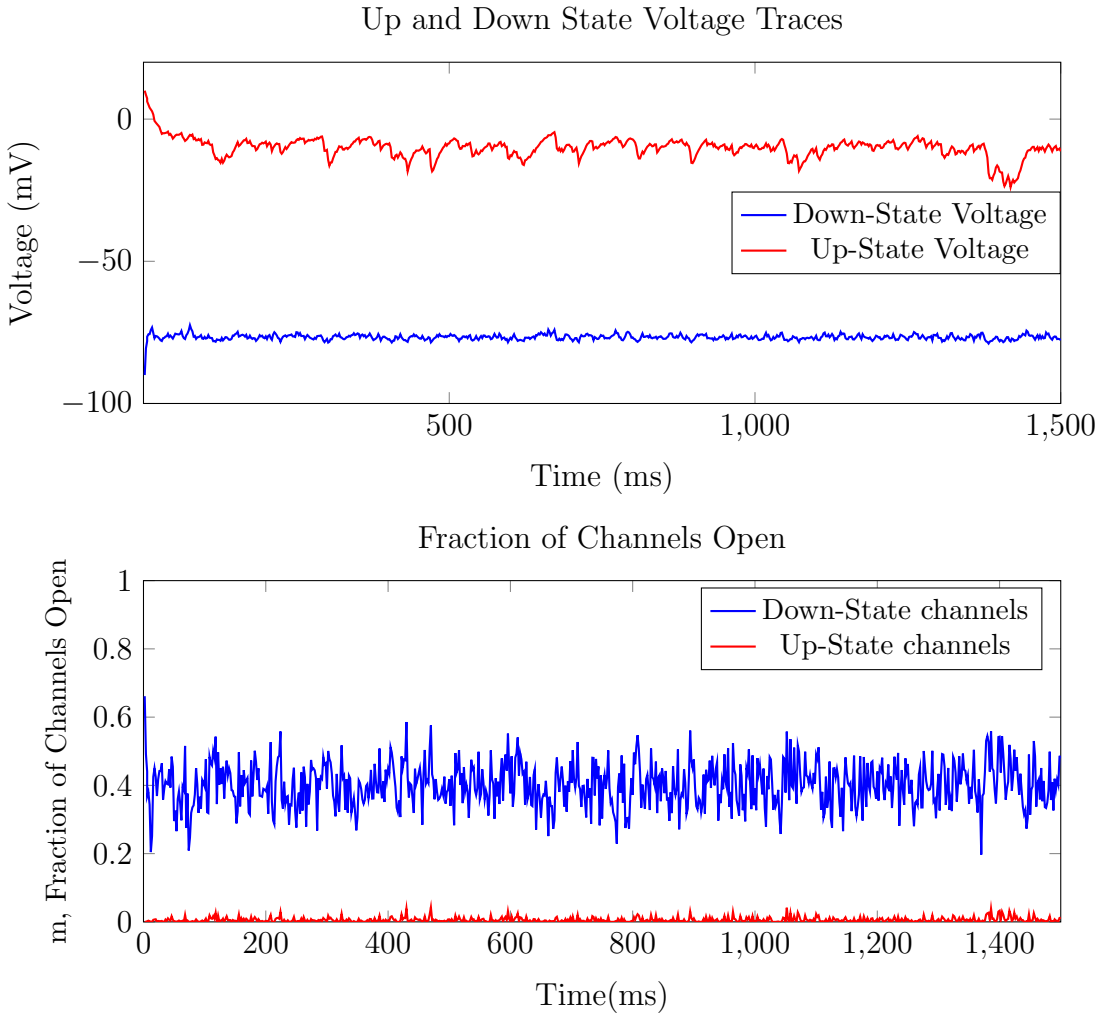

Figure 6: Top: Independent membrane potential voltage simulations for the two steady resting membrane potentials. Note that each trace corresponds to a different neuron simulation. The variance in the down-state (blue) is 0.90 mV^2. The variance in the up-state (red) is 13.26 mV^2. Bottom: Fraction of channels open during the up-state (red) and down-state (blue). Notice that increased channel noise in the down-state is not enough to cause larger membrane potential fluctuations. The high-conductance slope dampens the noise created by the channels.

4.2.2 Ranging The Kir Current

Our next step is to range the Kir current parameters. Bringing the max I_{Kir} conductance down would also decrease the difference between the two steady-state's conductances. Again, this allows the internal channel noise to have more of an influence on the down-state fluctuation amplitudes. It is also possible that increasing the max I_{Kir} conductance might increase the fluctuation amplitudes in the down-state. If I_{Kir} has a larger influence on the membrane potential, the channel noise would have a larger impact on the membrane potential as well. We tested different values for g_{Kir} and E_{Kir}, and also ran simulations in conjunction with

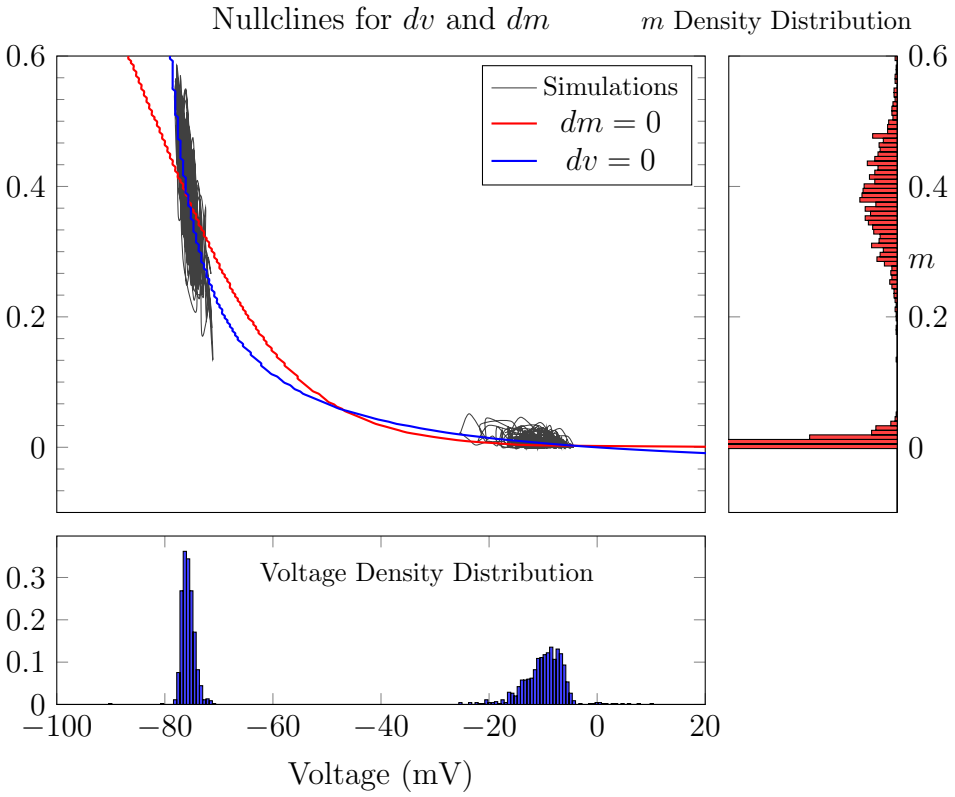

Figure 7: Top Left: The phase plane for voltage (v) and the fraction of open channels (m). The colored lines are the nullclines. On these lines, the rate of change for the variable is 0. The points where these lines cross is a steady-state for the system. Two of these are stable steady-states and correspond to the two stable resting membrane potentials for the neuron. The black lines show the evolution of the variables during the two individual simulations over time. Top Right: A density distribution of the m variable for the two simulations. m clearly has a much larger variance while in the down-state, and changes very little while in the up-state. Bottom: The density distribution of the voltage for the two simulations. Despite larger channel noise, the down-state has smaller voltage fluctuations than the up-state.

ranging leak parameters (Figure 9). We found the conductances could still not be brought close together while keeping the current parameters within realistic amounts.

An issue with manipulating these current parameters is maintaining bistability in the neuron model. As we attempt to bring the high-conductance branch to a lower conductance value, we risk bringing the threshold voltage (responsible for separating the two resting potentials) too close to the down-state. If the down steady-state and the threshold are too close, the window for voltage fluctuations will be too small. Any voltage fluctuations worth studying would be larger than the threshold and the membrane potential would move to the up-state. The bistablility in the system would be impractical and impossible to study.

After trying a range of values for the current conductances over the realistic physiological spectrum, we found this would most likely not be enough to evoke the reverse behavior from the model. The two resting membrane potential conductances could not be brought close enough together with these parameter shifts alone.

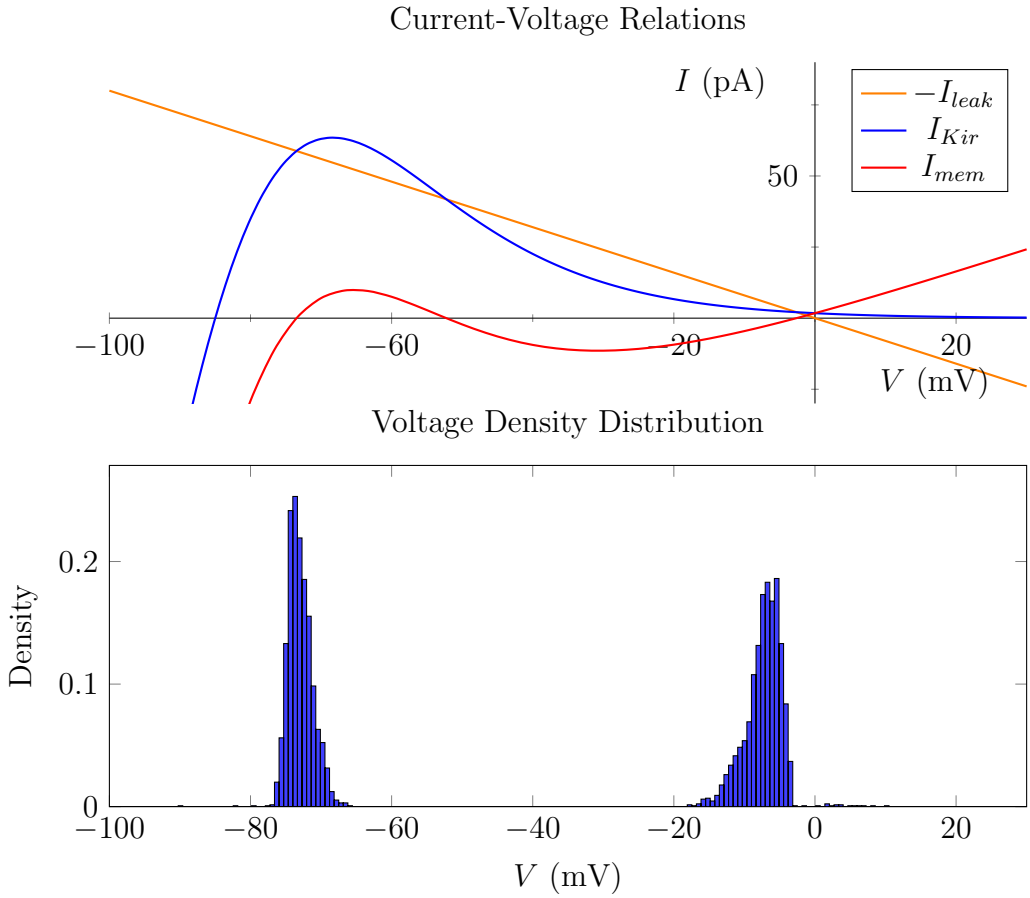

Figure 8: Top: The current voltage relations for I_{Kir} and I_{leak}, including the strengthened leak current. The leak conductance has been increased to $g_{leak} = 0.8$ pS. The I_{leak} I-V curve has been inverted across the x-axis. This allows for a better view of the two current interactions. Notice that in I_{mem} the high-conductance state's slope has decreased. This brings the conductances of the two states closer together. Bottom: The voltage density distribution for the simulations. The variance of the down-state is 3 mV^2. The variance of the up-state is 7.1 mV^2. The up-state still has larger membrane potential fluctuations.

4.2.3 Ranging The Number of Channels

Rather than trying to decrease the difference between the two resting membrane potentials conductances, we could increase the internal noise by decreasing the number of channels. With fewer channels, we expect the channel noise to increase. Fewer channels will lead to larger fluctuations away from the expected fraction of open channels. The increased channel noise in the membrane potential might be enough to overcome the noise-dampening influence of the high-conductance state. We decreased the number of channels for the voltage-gated IKR current and we found what we expected: increased channel noise and increased membrane potential noise. However, the channel noise was still larger in the high-conductance state. The decrease in the number of channels had an effect on both states. The up-state channel noise also increased, and the voltage fluctuations were still larger in low-conductance

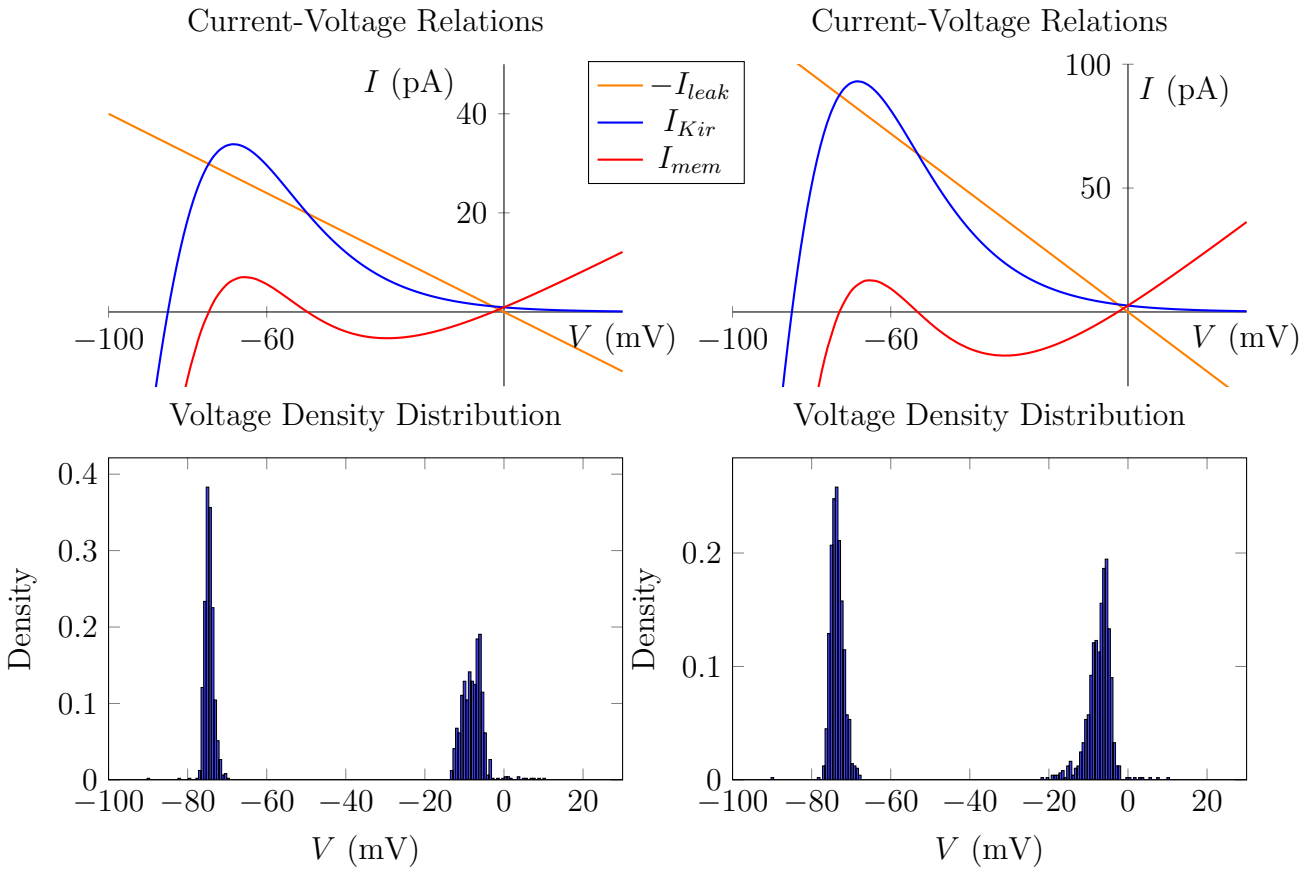

Figure 9: Top Left: I-V relation for smaller leak and potassium conductances. g_L is set to .4 pS and g_{Kir} is set to 9 pS. The conductances for the two steady-states are brought closer together. It is clear to see here how increasing the leak (or decreasing potassium) too much will disturb the bistability of the neuron. Bottom Left: Voltage density distribution for the smaller leak and potassium conductances. Down-state variance is 1.3 mV^2 and up-state variance is 6.3 mV^2. The sizes of the fluctuations in the two states were not brought close enough together. Top Right: I-V relation for larger leak and potassium conductances. g_L is set to .9 pS and g_{Kir} is set to 22 pS. With a stronger potassium current, the channel noise will have a larger impact on the down-state. Bottom Right: Voltage density distribution for the larger leak and potassium conductances. Down-state variance is 2.7 mV^2 and up-state variance is 8.8 mV^2.

state.

4.3 Augmenting the Leak Current

At this point we began to rework our simple model to account for more complexity in the currents. We accomplished this by augmenting the leak current to be slightly voltage dependent. We used the structure of a Goldman equation (Goldman, 1943) to make the leak current outward rectifying. An outward rectifying current is one that passes current more easily in the outward direction. The current has a stronger hyperpolarizing force,

and a weaker depolarizing force. This increases the membrane conductance in the up-state and decrease the membrane conductance in the down-state. The goal is again to bring the two resting membrane potential conductances closer together, in order to allow the internal channel noise to play the leading roll in designating the larger fluctuation amplitude for either state.

The new leak equation has the form:

$$I_{leak} = g_{leak} z^2 v \frac{F}{RT} \frac{[O] - [I] exp(-zv\frac{F}{RT})}{1 - exp(-zv\frac{F}{RT})}, \tag{11}$$

where z is the valence of the ion, F is Faraday's constant, R is the ideal gas constant, T is the temperature in kelvins, $[O]$ is the concentration of ions outside the neuron, and $[I]$ is the concentration of ions inside the neuron. The current voltage relation is visualized in Figure 10.

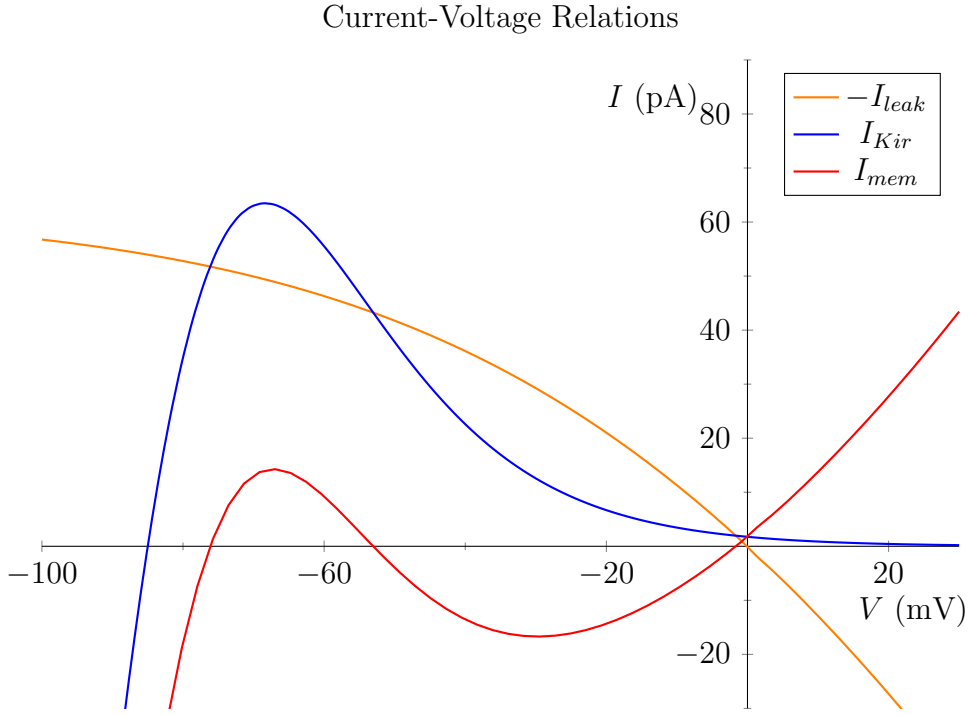

Figure 10: The current voltage relations with a new voltage dependent leak equation. The leak curve has been in inverted across the x-axis to help visualize the interactions between the leak current and the I_{Kir} current. Notice how similar the conductances became at each steady-state.

We ran simulations with the new leak current, and with the changes the low-conductance state still had larger fluctuations. Although, it is worth noting here that the differences in the membrane fluctuations in these simulations were closer than another other run. We tried to exaggerate the outward rectifying leak further by increasing the $[I]$:$[O]$ ratio. However, this manipulation did not have the desired result. The curve would not get more extreme for larger ratios. We found we could exaggerate the bend of the curve by lowering $\frac{F}{RT}$ from

25 mV to 7 mV. This brought the conductances together, however it also brought the model far outside realistic parameters.

5 Conclusions

Our findings suggest the stochastic gating of the ion channels is not enough to create larger membrane potential fluctuations in the high-conductance state than in the low-conductance state. In a simple bistable neuron model that exhibits an inward-rectifying current (I_{Kir}) and a leak current, we found the noise generated by the stochastic gating of the voltage-gated ion channels was not able to overcome the voltage-dependent membrane conductance in the down-state. This conclusion remains supported after extensive realistic parameter ranging studies.

We referenced before that in neurophysiology studies on plateau potentials, the size of the fluctuations is a major interest to investigators because they drive the transitions between the states. Researchers occasionally observe larger fluctuations in what we have been calling the high-conductance state (Hounsgaard et al., 1988). This phenomenon is not explained by the idea that the size of the membrane potential fluctuations in each steady-state arises from the different membrane conductance for each steady-state. However, we showed that this behavior is most likely not caused by internal noise generated by the stochastic gating of the ion channels, as has been suggested. The unexpected behavior of larger fluctuations in the high-conductance state is probably a result of more complicated characteristics of the neuron that were not replicated in our simple model. We explored a wide range of parameters, but we did not observe the internal voltage-gated channel noise creating larger membrane potential fluctuations in the high-conductance state than in the low-conductance state.

One possibility for the counterintuitive behavior is the existence of several more interacting intrinsic currents in the neuron. It is unlikely that a neuron should exhibit only the two types of currents we included in our model. Generating action potentials alone would require a minimum of two additional currents. We don't know exactly how the currents present in these neuron will interact, and it is possible that those interactions are responsible for the unexplained membrane potential fluctuations in the high-conductance state. We approached something similar to this environment with the augmented leak current. With a more complicated leak current, the variances in the voltage between the plateau potential and the down-state were closer together than in any other scenario. This represents the possibility of additional currents creating more complicated behavior, unexplained by our model. Another possibility to explore is the neuron's synaptic connections. Perhaps the neuron receives a large increase in post-synaptic activity during its high-conductance state, due to the neuron's network architecture. In any case, we showed that, in a simple bistable neuron model with I_{Kir} and a leak current, stochastic channel gating noise was not enough to create larger membrane potential fluctuations in the high-conductance state than in the low-conductance state over realistic parameters.

6 Future Directions

An obvious next step for the project would be to create a simple bistable neuron model with the L-type calcium current and a leak current. The appeal of this project is it is the mirror system to the one studied in this thesis. The high and low conductance branches are switched and the gating dynamics of the calcium current are also reversed compared to the inward-rectifying potassium current. The calcium current is on during depolarization. An analysis into this other system is the next step of the project. The observations from this system would help to confirm some of our conclusions in this thesis. This type of project would have important results and would not take a long time to implement. Most of the framework for the simulations was already built in this thesis. Changing the types of currents in the model would only require research into the parameters and the equations necessary to model them.

Another direction we would like to take the project is to nondimensionalize the system of ODEs. This process removes units from the equations, while still preserving the desired characteristics of the system. This would ultimately lead to fewer parameters in the ODEs. Less parameters in the equations means we could run parameter studies more efficiently and more accurately, as we could compare more parameter values with less computational effort. Using this approach, we might be able to definitively show that there exists no parameter ranges where the counterintuitive results are possible.

References

Cervera, J., Alcaraz, A., and Mafe, S. (2014). Membrane potential bistability in nonexcitable cells as described by inward and outward voltage-gated ion channels. *The Journal of Physical Chemistry B*, 118(43):12444–12450.

Chow, C. C. and White, J. A. (1996). Spontaneous action potentials due to channel fluctuations. *Biophysical journal*, 71(6):3013–3021.

Fox, R. F. (1997). Stochastic versions of the hodgkin-huxley equations. *Biophysical journal*, 72(5):2068–2074.

Goldman, D. E. (1943). Potential, impedance, and rectification in membranes. *The Journal of general physiology*, 27(1):37–60.

Higham, D. J. (2001). An algorithmic introduction to numerical simulation of stochastic differential equations. *SIAM review*, 43(3):525–546.

Hodgkin, A. L. and Huxley, A. F. (1952). A quantitative description of membrane current and its application to conduction and excitation in nerve. *The Journal of physiology*, 117(4):500.

Hounsgaard, J., Hultborn, H., Jespersen, B., and Kiehn, O. (1988). Bistability of alpha-motoneurones in the decerebrate cat and in the acute spinal cat after intravenous 5-hydroxytryptophan. *The Journal of physiology*, 405(1):345–367.

Hounsgaard, J. and Kiehn, O. (1989). Serotonin-induced bistability of turtle motoneurones caused by a nifedipine-sensitive calcium plateau potential. *The Journal of physiology*, 414:265.

Keizer, J. (1987). *Statistical thermodynamics of nonequilibrium processes*. Springer-Verlag.

Kiehn, O. and Eken, T. (1998). Functional role of plateau potentials in vertebrate motor neurons. *Current opinion in neurobiology*, 8(6):746–752.

Newell, E. W. and Schlichter, L. C. (2005). Integration of k+ and cl–currents regulate steady-state and dynamic membrane potentials in cultured rat microglia. *The Journal of physiology*, 567(3):869–890.

Smith, G. D. (2002). Modeling the stochastic gating of ion channels. In *Computational cell biology*, pages 285–319. Springer.

Wang, X., Weinberg, S. H., Hao, Y., Sobie, E. A., and Smith, G. D. (2015). Calcium homeostasis in a local/global whole cell model of permeabilized ventricular myocytes with a langevin description of stochastic calcium release. *American Journal of Physiology-Heart and Circulatory Physiology*, 308(5):H510–H523.

White, J. A., Rubinstein, J. T., and Kay, A. R. (2000). Channel noise in neurons. *Trends in neurosciences*, 23(3):131–137.

Williams, S. R., Tóth, T. I., Turner, J. P., Hughes, S. W., and Crunelli, V. (1997). The windowcomponent of the low threshold ca2+ current produces input signal amplification and bistability in cat and rat thalamocortical neurones. *The Journal of Physiology*, 505(3):689–705.

Wilson, C. J. and Kawaguchi, Y. (1996). The origins of two-state spontaneous membrane potential fluctuations of neostriatal spiny neurons. *Journal of neuroscience*, 16(7):2397–2410.

A Appendices

A.1 First appendix

```
close all;
clear;
clc;

%% Parameters
% System settings
ncell   = 2;          % number of simulations/cells
Nchanl  = 15;         % number of channels in Ikir
```

```
% Initial values
V_cell  =  linspace(-90,20,ncell);     % Initial Voltages

% Time Parameters
tMin    = 0;
tMax    = .2e3;
tStep   = .1;
times   = tMin:tStep:tMax-tStep;

% Neuron Paremeters
C       = 2;                % Membrane capacitance
gleak   = 0.45;             % Leak max conductance
Eleak   = 10;               % Reversal potential for leakage current

gKir    =  6;              % Potassium current max conductance
EKir    = -100;              % Reversal potential for potassium current
sigma_Kir = 12.4;           % Rate at which conductance changes with voltage
Vhalf_Kir = -81.7;          % Voltage when the conductance is half maximal

i0    =  0;                 % Applied current
i1    =  1;                 % Fluctuating applied current amplitude
i1w    = 1.0;                % Fluctuating applied current period

%% Equations
Ileak = @(V)   (gleak .* (V-Eleak));         % leak current
IKir  = @(V,m) (gKir .* m .*(V-EKir));       % IR potassium current

minf = @(V) (1./(1+exp((V-(Vhalf_Kir))./sigma_Kir)));  % SS of IRK channel
Taum = @(V) 1;

% Markov state model stuff
alpha = @(V)    minf(V)/Taum(V);     % rate a channel opens
beta  = @(V)    (1-minf(V))/Taum(V); % rate a channel closes
gamma = @(V,m)  (alpha(V).*(1-m) + beta(V).*(m))/Nchanl;   % variance
noise = @(V,m)  randn.*sqrt(gamma(V,m)./tStep);       % noise term

V = zeros(ncell,length(times));      % Actually setting initial conditions
V(:,1) = V_cell;

m = zeros(ncell,length(times));
m(:,1) = minf(V(:,1));

% Euler's method for solving a differential equation
for i = 1:length(times)-1
    V(:,i+1) = V(:,i) + tStep * ((i0 + i1*cos(i1w*i)   ...
```

```
            - Ileak(V(:,i)) - IKir(V(:,i), m(:,i)))/C);
        m(:,i+1) = m(:,i) + tStep * (alpha(V(:,i)).*(1-m(:,i)) ...
            - beta(V(:,i)).*m(:,i) + noise(V(:,i),m(:,i)));
        m(:,i+1) = min(1,m(:,i+1));
        m(:,i+1) = max(0,m(:,i+1));
end

%% Calculate Voltage Variances
%NetI = IKir(Vimage,mimage) - Ileak(Vimage);
Threshold = -59;
Vlow = V<Threshold; %ideally this threshold would be set by the script
Vlow = Vlow .* V;
Vlow = Vlow(Vlow~=0);

Vhigh = V>Threshold;
Vhigh = Vhigh .* V;
Vhigh = Vhigh(Vhigh~=0);

%% Figures
figure('DefaultAxesFontSize',15,'Position',[40 40 1350 750]);
subplot(2,2,1);
plot(times,V);
title('Potassium and Leak Voltage Trace');
ylabel('Voltage, (mV)');
xlabel('Time (ms)');
legend('Low Voltage','HighVoltage')


%figure(2)
subplot(2,2,2)
plot(times,m,'LineWidth',2);
axis([0 tMax 0 1])
xlabel('Time(ms)');ylabel('Fraction of channels open');
title('Fraction of channels open')
legend('Low Voltage trace channels','High Voltage trace channels')

current_and_dvdt_images;


subplot(2,2,4)
plot(Vimage,minf(Vimage),'LineWidth', 2);
xlabel('Voltage (mV)');
ylabel('Proportion of channels open');
title('Kir Channels open vs Cell Voltage')
axis([-120 40 0 1]);
```